EARTHQUAKE ENGINEERING AND STRUCTURAL DYNAMICS
Earthquake Engng. Struct. Dyn. **28**, 235–254 (1999)

A NEW METHOD OF REDUCED-ORDER FEEDBACK CONTROL USING GENETIC ALGORITHMS

YOON-JUN KIM† AND JAMSHID GHABOUSSI*,‡
Department of Civil Engineering, University of Illinois at Urbana-Champaign, Urbana, IL 61801, U.S.A.

SUMMARY

Genetic Algorithms (GAs) have been applied as an effective optimization search technique in various fields, including the field of control design. In this paper, a new control method using GAs is proposed to attenuate the responses of a structure under seismic excitation. The proposed controller uses the state-space reconstruction technique based on the embedding theorem to obtain full-state performance from the available reduced order feedback. The parameters of the new controller are optimized using GAs. The proposed GA-based control method is verified on a benchmark problem—active mass driver system, and the results are compared with other control methods. The robustness of the proposed control method is also examined.

KEY WORDS: active control; genetic algorithms; dynamics; earthquake; structures; state space reconstruction

INTRODUCTION

Most control design methods are based on the optimization technique of maximizing the performance using less control energy under certain constraint. The optimization procedure can be described briefly as tuning the parameters of the controller. Most optimization methods used in control design are traditional gradient-based search methods. With this approach, however, there are difficulties associated in selecting the suitable continuous differentiable cost function and in considering non-linearities.[1] Unlike traditional optimization methods, Genetic Algorithms (GAs) efficiently find an optimal solution from the complex and possibly discontinuous solution space.

GAs have been applied as an effective search technique to various fields of optimization problems.[2] In the field of control design, for example, GAs have been successfully applied to obtain gains for the optimal controller,[3] tune the weights of neuro-controllers,[4] and scale parameters of fuzzy controllers.[5]

For the control of the civil structures, a new reduced-order feedback control method using GAs is proposed in this paper. The proposed method uses the reduced-order feedback which can be

* Correspondence to: Janshid Ghaboussi, Department of Civil Engineeering, University of Illinois at Urbana-Champaign, Urbana, IL 61801, U.S.A. E-mail: jghabous@uiuc.edu
† Graduate Research Assistant
‡ Professor of Civil Engineering

Contract/grant sponsor: National Science Foundation; Contract/grant number: CMS-95-003209

CCC 0098–8847/99/030235–20$17·50

Received 22 March 1997
Revised 20 June 1998

measured directly with a limited number of sensors. To obtain the full-state performance, the state-space reconstruction method is applied. The state-space reconstruction method is based on the embedding theorem (Takens 1981) which describes that the states reconstructed in the delay coordinates can characterize the dynamical information of the original state space. With this method, the system states are reconstructed from the observed time-series data. The proposed controller uses the reconstructed state space as the feedback and the parameters of the controller are optimized by GAs.

The proposed method has been used on a benchmark problem.[6] Two controllers have been developed—one without sensor noise (Case A), and another with sensor noise (Case B). Both controllers work with four sensors measuring the absolute accelerations of three floors and AMD mass as a feedback. The results have been compared with the results of several other control methods.[6–10] The robustness of both controllers has also been examined.

GENETIC ALGORITHMS

Originally, GAs have been developed to explain and simulate the adaptive processes of biological systems, i.e. natural evolution. In GAs organisms or chromosomes evolving under a certain environment are represented by bit strings. Each string consists of several genes, and the combination of consecutive genes in the string represents a parameter of the problem to be optimized. Strings evolve over generations to adapt to a given environment using genetic algorithm operators.

There are three genetic algorithm operators: selective reproduction, cross-over and mutation. In every generation, a set of strings is selected into the mating pool based on their relative fitness. The fitter strings are given more chance of passing their genes into the next generation. This process of natural selection, i.e. survival of the fittest is operated by selective reproduction. New strings are created by exchanging the genes between two old strings (cross-over). Mutation operator is applied at a specified low rate to change the randomly selected genes in the new generation. As Goldberg indicates,[2] 'While randomized, GAs are no simple random walk. They efficiently exploit historical information to speculate on new search points with expected improved performance'. GAs are probabilistic searching techniques which explore the new searching space as well as keep the historical information of the searching space.

GAs are very simple but powerful methods compared with the traditional gradient-based search methods because GAs do not need the reformulation of the problem to search a non-linear and non-differentiable space. The flexibility in the formulation of the fitness function is also one of the advantages of GAs. The fitness function can be formulated as a polynomial function of the output of the system to be optimized. Therefore, by using GAs, multiple optimal design criteria can be considered by simply including them in the fitness function.

GA-BASED REDUCED-ORDER FEEDBACK CONTROL

This section describes a new state space reconstruction technique to obtain the full-state performance from reduced-order feedback as well as the control law used in the proposed GA-based controller.

State-space reconstruction by embedding

In practice, the full-state information is not always available. Also, the measurement of displacements and velocities of a structure during an earthquake is difficult. To approach the full-state performance, it is necessary to estimate the full-state space from the reduced order feedback. The traditional optimal control methods use the observer to estimate the state.

A new method to estimate the original state space from observed time series is developed in this study. The method is based on Takens' embedding theorem,[11] which states that observed time-series data can be used to reconstruct the state space of the underlying system. Let us define $\mathrm{W}^n(t)$ as the n-dimensional reconstructed state space vector at time step t. $\mathbf{W}^n(t)$ is composed of one-dimensioinal observed time series $w(t)$ with time delay τ as follows.

$$\mathbf{W}^n(t) = \{w(t)w(t-\tau) \cdots w[t-(n-1)\tau]\}^{\mathrm{T}} \tag{1}$$

The reconstructed state-space $\mathbf{W}^n(t)$ is not the same as the original state space. However, it can characterize the dynamical properties (the attractor in the phase space) of the original system for a sufficiently large value of n. When the dimension of the underlying state space producing the time series is l, Takens has suggested a value of $n > 2l$. However, the embedding often works well for smaller values of n.[12] The optimum value of the time delay τ is still an open question. Generally, the optimum value for τ depends on the statistical correlation between the samples. Larger values of τ can be used when the statistical correlation is high.[12]

For the benchmark problem described in the next section, we have the vector of the observed time-series $\mathbf{w}(t)$ which contains the measurements from sensors. The dimension of the reconstructed state space will be equal to $s \times n$ in this case, where s is the number of system states measured from sensors.

$$\mathbf{W}^{s\times n}(t) = \{\mathbf{w}(t)\mathbf{w}(t-\tau) \cdots \mathbf{w}[t-(n-1)\tau]\}^{\mathrm{T}} \tag{2}$$

Proposed GA-based control method

The following equation is the control law which is used in the proposed GA-based control method. In this equation the control signal increment $\Delta\mathbf{u}$ is a function of the reconstructed states of control input vector $\mathbf{u}$ and the vector of measured responses $\mathbf{y}$.

$$\Delta\mathbf{u}(t) = f[\mathbf{u}(t-\tau), \mathbf{u}(t-2\tau), \ldots\ldots, \mathbf{u}(t-m\tau), \mathbf{y}(t), \mathbf{y}(t-\tau), \ldots\ldots, \mathbf{y}(t-(n-1)\tau]] \tag{3}$$

Figure 1 shows the flow diagram for the design of the GA-based controller. The fitness value of each controller is determined directly from the controlled responses of the structure. The fitness function for the evaluation of each controller's fitness value will be described in detail later.

BENCHMARK PROBLEM, ACTIVE MASS DRIVER SYSTEM

The proposed GA-based control method has been evaluated on a benchmark problem. The structure considered in the benchmark problem is a scale model of a three storey building using an active mass driver as a control device. State-space parameters of this structural system, including the actuator and sensor dynamics, have been obtained from an experiment.[13] More details on the benchmark problem can be found in Reference 6.

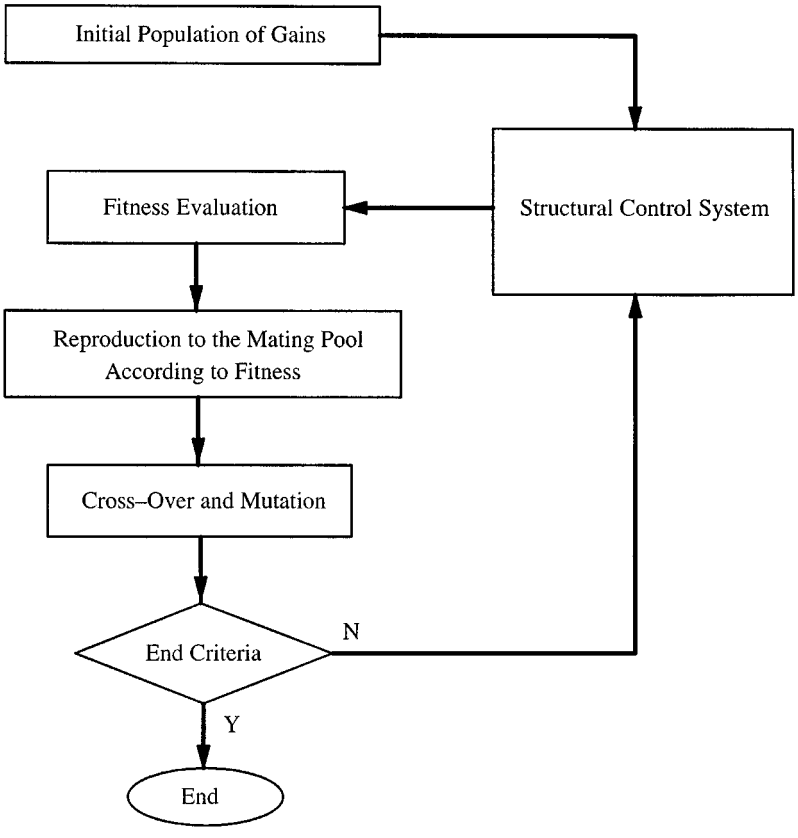

Figure 1. Flow diagram for GA-based controller design

Evaluation model

A linear time-invariant state-space representation of the structural system for the benchmark problem is described by the following equations.

$$\dot{\mathbf{x}} = \mathbf{A}\mathbf{x} + \mathbf{B}u + \mathbf{E}\ddot{x}_{\mathrm{g}} \tag{4}$$

$$\mathbf{y}_{\mathrm{m}} = \mathbf{C}_y\mathbf{x} + \mathbf{D}_y u + \mathbf{F}_y\ddot{x}_{\mathrm{g}} + \mathbf{v} \tag{5}$$

$$\mathbf{z} = \mathbf{C}_z\mathbf{x} + \mathbf{D}_z u + \mathbf{F}_z\ddot{x}_{\mathrm{g}} \tag{6}$$

In these equations $\mathbf{x}$ is the state vector composed of 28 state variables, $\ddot{x}_{\mathrm{g}}$ is the scalar ground acceleration, u is the scalar control input, $\mathbf{y}_{\mathrm{m}}$ is the vector of measurable responses, $\mathbf{z}$ is the vector of controllable responses, and $\mathbf{v}$ is the vector of sensor noises. Vectors $\mathbf{y}_{\mathrm{m}}$ and $\mathbf{z}$ are described by the following equations.

$$\mathbf{y}_{\mathrm{m}} = \{x_{\mathrm{m}}\ddot{x}_{a1}\ddot{x}_{a2}\ddot{x}_{a3}\ddot{x}_{am}\ddot{x}_{\mathrm{g}}\}^{\mathrm{T}} \tag{7}$$

$$\mathbf{z} = \{x_1 x_2 x_3 x_m \dot{x}_1 \dot{x}_2 \dot{x}_3 \dot{x}_m \ddot{x}_{a1}\ddot{x}_{a2}\ddot{x}_{a3}\ddot{x}_{am}\}^{\mathrm{T}} \tag{8}$$

In these equations, x_i is the displacement of the ith floor relative to the ground, $\dot{x}_i$ is the velocity of the ith floor relative to the ground, x_m is the displacement of the AMD relative to the third floor, $\ddot{x}_i$ is the absolute acceleration of the ith floor, and $\ddot{x}_{am}$ is the absolute acceleration of the AMD mass. Inter-storey drifts are defined as $d_1(t) = x_1(t)$, $d_2(t) = x_2(t) - x_1(t)$, $d_3(t) = x_3(t) - x_2(t)$.

The coefficient matrices of state equations in equations (4)–(6) were determined by the system identification of the model building in the Structural Dynamics and Control/Earthquake Engineering Laboratory (SDC/EEL) at the University of Notre Dame and represent the input–output behaviour of the structure system up to 100 Hz. The model includes actuator/sensor dynamics and control-structure interaction.

Control constraints

Control constraints are placed on the system for a realistic numerical simulation. The primary constraints (hard constraints) depend on the physical characteristics of the experimental setup and the capacity of the actuator. The RMS constraints and the peak response constraints are listed in equations (9) and (10), respectively. In equation (9) σ represent the RMS value of its subscript.

$$\sigma_u \leqslant 1 \text{ V}, \sigma_{\ddot{x}_{am}} \leqslant 2 \text{ g} \text{ and } \sigma_{x_m} \leqslant 3 \text{ cm} \tag{9}$$

$$\max|u| \leqslant 3 \text{ V}, \max|\ddot{x}_{am}| \leqslant 6 \text{ g} \text{ and } \max|x_m| \leqslant 9 \text{ cm} \tag{10}$$

The additional constraints (control implementation constraints), which depend on the sensors and the controller computer, are as follows.

1. Available measurements to determine the control action are **y** in equation (7) which also includes the measured ground acceleration.
2. Sampling time is 0·001 s.
3. A computation time delay of 200 μs is used.
4. The A/D and D/A converters on the digital controller have a 12 bit precision and a span of $\pm$ 3 V.
5. The measurement noises with RMS value of 0·01 V which is approximately 0·3 per cent of the full span of the A/D converters are considered.

CONTROLLER DESIGN

GA-based controller

In order that the results of the benchmark problem using the GA-based controller can be compared with the results from other optimal control methods, we have chosen to use four sensors, similar to other optimal control methods applied to the benchmark problem. Absolute accelerations of three floors, $\ddot{x}_{a1}$, $\ddot{x}_{a2}$, $\ddot{x}_{a3}$, and the absolute acceleration of AMD mass, $\ddot{x}_{am}$, are measured by four accelerometers. The feedback vector $\mathbf{y}(t)$ contains the following four sensor readings at time t.

$$\mathbf{y}(t) = \{\ddot{x}_{a1}\, \ddot{x}_{a2}\, \ddot{x}_{a3}\, \ddot{x}_{am}\} \tag{11}$$

By using the reconstructed state feedback, we are using the current vector of sensor reading $\mathbf{y}(t)$ plus previous samples of sensor readings. Therefore, the dimension of the reconstructed state space of the four sensor feedback will be equal to $4 \times n$ with $n - 1$ previous time histories.

$$\mathbf{Y}^{4\times n}(t) = \{\mathbf{y}(t)\mathbf{y}(t-\tau) \cdots \mathbf{y}(t-[n-1]\tau)\}^{\mathrm{T}} \tag{12}$$

The proposed controller also uses previous time histories of control signals as a feedback. One role of this feedback is to make the control signal not to deviate too much from the zero signal in the incremental form of the control law used in this study as in equation (3).

$$\mathbf{U}^{m}(t-\tau) = \{u(t-\tau)u(t-2\tau) \cdots u(t-m\tau)\}^{\mathrm{T}} \tag{13}$$

Currently, there is no rigorous method to determine the values of m and n. As the role of m and n in the performance of the reconstructed state feedback becomes clearer with further research, it will be possible to develop more rigorous guidelines for their calculation. For this study we have chosen to use a trial and error method. Figure 2 shows the fitness transition curve with respect to the dimension of the reconstructed state space. It is seen from this figure that the 7-dimensional ($m = 3, n = 1$), 19-dimensional ($m = 3, n = 4$), and 23-dimensional ($m = 3, n = 5$) cases of the reconstructed state space are compared. There are sudden improvements in the control performance which can be distinguished in the early generations (less than 100th generation). As the dimension of the reconstructed state space n increases, the fitness of the controller improves as shown in the figure. In the remainder of this study, we have used the 23-dimensional reconstructed state space which consists of 20-dimensional reconstructed state space vector $\mathbf{Y}^{4\times 5}(t)$ and the 3-dimensional reconstructed state-space vector $\mathbf{U}^{3}(t-\tau)$. They are described in following equations:

$$\mathbf{Y}^{4\times 5}(t) = \{\mathbf{y}(t)\mathbf{y}(t-\tau) \cdots \mathbf{y}(t-4\tau)\}^{\mathrm{T}} \tag{14}$$

$$\mathbf{U}^{3}(t-\tau) = \{u(t-\tau)u(t-2\tau)u(t-3\tau)\}^{\mathrm{T}} \tag{15}$$

Using the feedback in equations (14) and (15), the control input is calculated from equation (16) with the additional constraint from the saturation of the actuator which requires that $|u| \leqslant +3$ V as a limit. Figure 3 shows the block diagram of the proposed controller.

$$u(t) = u(t-\tau) + \Delta u(t), \text{ where } \Delta u(t) = \mathbf{G}_{\mathrm{R}} \begin{Bmatrix} \mathbf{Y}^{4\times 5}(t) \\ \mathbf{U}^{3}(t-\tau) \end{Bmatrix} \tag{16}$$

The controller gain matrix $\mathbf{G}_{\mathrm{R}}$ for reconstructed state space feedback $\mathbf{Y}^{4\times 5}(t)$ and $\mathbf{U}^{3}(t-\tau)$ has 23 elements as follows. The elements of the gain matrix $\mathbf{G}_{\mathrm{R}}$ are optimized through evolution by using GAs.

$$\mathbf{G}_{\mathrm{R}} = [\mathbf{G}_1 \;\; \mathbf{G}_2] \tag{17}$$

$$\mathbf{G}_1 = [g_1 g_2 \cdots g_{19} g_{20}], \quad \mathbf{G}_2 = [g_{21} g_{22} g_{23}]$$

The number of operations (a multiplication followed by an addition) needed for determining $u(t)$ in the control computer is important. It determines the computational time delay. The number of operations in equation (16) is 23. This is far fewer than the number of operations needed in most other control methods, including the discrete-time feedback compensator with 12-state feedback.[6]

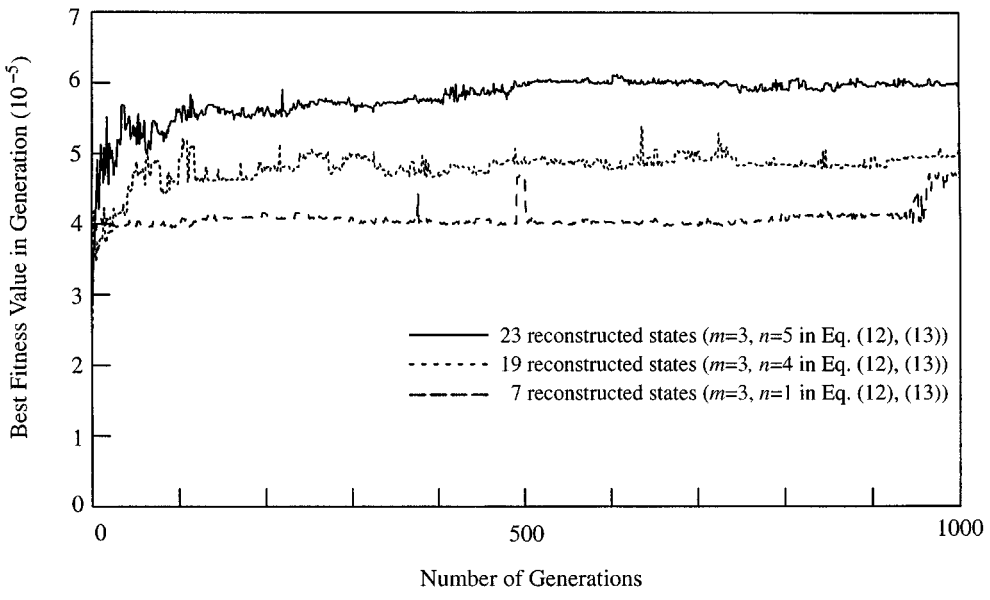

Figure 2. Fitness transition curve with respect to dimension of reconstructed state space (Case A)

Fitness function

The fitness function F is a non-linear polynomial which consists of powered products of the normalized peak and RMS values of the responses of floors and the AMD. Each criterion of C_1–C_5 has been designed to converge to 1·0 when the corresponding system response is reduced to zero.

$$F = \frac{C_{\text{ref}}}{C_{\text{T}}} \tag{18}$$

$$C_{\text{T}} = \prod_{i=1,5} C_i \tag{19}$$

$$C_1 = \prod_{i=1,3} \left(1 + \frac{|\ddot{x}_{\text{ai}}|_{\max}}{\beta_i}\right)^{a_i} \cdot \left(1 + \frac{P(|\ddot{x}_{\text{am}}|_{\max}}{\beta_m}\right)^{a_m} \tag{20}$$

$$C_2 = \prod_{i=1,3} \left(1 + \frac{|x_i|_{\max}}{\delta_i}\right)^{\gamma_i} \cdot \left(1 + \frac{P(|x_m|_{\max})}{\delta_m}\right)^{\gamma_m} \tag{21}$$

$$C_3 = \prod_{i=1,3} \left(1 + \frac{\sigma_{\ddot{x}_{\text{ai}}}}{\zeta_i}\right)^{\varepsilon_i} \cdot \left(1 + \frac{\sigma_{\ddot{x}_{am}}}{\zeta_m}\right)^{\varepsilon_m} \tag{22}$$

$$C_4 = \prod_{i=1,3} \left(1 + \frac{\sigma_{x_i}}{\theta_i}\right)^{\eta_i} \cdot \left(1 + \frac{\sigma_{x_m}}{\theta_m}\right)^{\eta_m} \tag{23}$$

$$C_5 = \left(1 + \frac{\sigma_u}{\omega}\right)^{\psi} \tag{24}$$

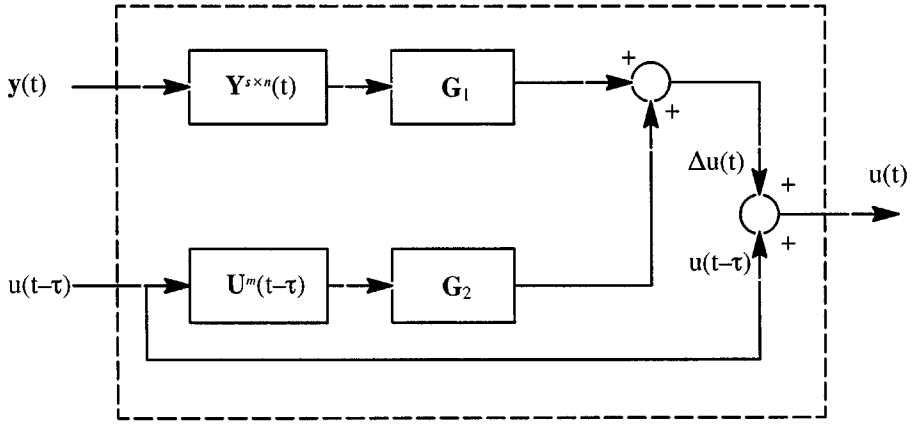

Figure 3. Block diagram lf GA-based controller (Cases A and B)

For the evaluation of the fitness, peak accelerations, peak displacements, RMS accelerations and RMS displacements of the three floors and active mass driver and RMS value of the control signal are used as parameters of the cost function in equations (20)–(24). The denominators $\beta, \delta, \zeta, \theta$, and ω are the normalization factors, and powers, $\alpha, \gamma, \varepsilon, \eta$, and ψ are the exponential weight factors used to adjust the weight of responses which are to be reduced according to the control objective. In this study the factors are chosen by trial and error as follows: $\beta_i = 2.0$, $\beta_m = 1{\cdot}0$, $\delta_i = \delta_m = 1{\cdot}0$, $\zeta_i = 2{\cdot}0$, $\zeta_m = 1{\cdot}0$, $\theta_i = \theta_m = 1{\cdot}0$, and $\omega = 1{\cdot}0$ for normalization, and $\alpha_i = 1{\cdot}0$, $\alpha_m = 3{\cdot}0$, $\gamma_i = 1{\cdot}0$, $\gamma_m = 2{\cdot}0$, $\varepsilon_i = \varepsilon_m = 1{\cdot}5$, $\eta_i = \eta_m = 1{\cdot}0$, and $\psi = 1{\cdot}0$ for exponential weight facdtors. Equation (19) shows the total cost, and the fitness is the inverse of the total cost as shown in equation (18) with a normalization factor C_{ref} ($= 1{\cdot}0$ in this study). Function P in equations (20) and (21) is the penalty function to be explained next.

Penalty function

The penalty function has been successfully used for solving the constrained optimization problem by several researchers.[1,14] In the early stages of evolution, the penalty function plays the role of confining the search space by adding a large penalty value to the cost function. As a result, the GA searches the fittest solution within the space that satisfies constraints after a few generations.

This penalty function is employed to impose the benchmark problem's hard constraints. Thus, the control strings which violate the constraints are assigned lower fitness values and thereby have less chance of passing their genes to the next generation. Consequently, the population of strings in GAs evolves toward satisfying those constraints. The following equations show the

penalty functions used on the benchmark problem. The penalty term 50 is used in this study.

$$P(|x_m|_{\max}) = \begin{cases} |x_m|_{\max} & \text{for } |x_m|_{\max} \leqslant 9 \text{ cm} \\ 50 & \text{for } |x_m|_{\max} > 9 \text{ cm} \end{cases} \tag{25}$$

$$P(|\ddot{x}_{am}|_{\max}) = \begin{cases} |\ddot{x}_{am}|_{\max} & \text{for } |\ddot{x}_{am}|_{\max} \leqslant 6 \text{ g} \\ 50 & \text{for } |\ddot{x}_{\mathrm{am}}|_{\max} > 6 \text{ g} \end{cases} \tag{26}$$

GA parameters

The binary coded simple GA[2] is employed to optimize feedback gains. Ten bits are used to represent each gain as a real number by mapping, making the string length equal to 230 bits. The population size was 50 and the evolution was continued up to 1000 generations. Genetic operators used are: fitness proportional (roulette wheel type) random reproduction, two point cross-over at a rate of 0·8 and mutation at a rate of 0·003.

EVALUATION CRITERIA

Root mean square and peak responses are used as the evaluation criteria of control efficiency. Ten criteria are defined in the benchmark problem,[6] and they are normalized by the corresponding worst–case responses of the third floor.

Root–mean-square responses to Kanai–Tajimi excitation spectrum

The first five evaluation criteria use root–mean-square responses to random excitation with a spectral density defined by the Kanai–Tajimi spectrum.

$$S_{\ddot{x}_g \ddot{x}_g}(\omega) = S_0 \frac{4\zeta_g^2 \omega_g^2 \omega^2 + \omega_g^4}{(\omega^2 - \omega_g^2)^2 + 4\zeta_g^2 \omega_g^2 \omega^2}, \quad S_0 = \frac{0{\cdot}03\zeta_g}{\pi\omega_g(4\zeta_g^2 + 1)} \tag{27}$$

The frequency ω_g and damping ratio ζ_g of the bedrock-ground connection are given in the following ranges: 20 rad/s $\leqslant \omega_g \leqslant$ 120 rad/s, 0·3 $\leqslant \zeta_g \leqslant$ 0·75. S_0 is the spectral density, chosen for the RMS value of the ground motion to be 0·12 g.

The first criterion, J_1, represents the controller's ability to minimize the maximum RMS inter-storey drift, and J_2 is calculated from the maximum RMS absolute acceleration.

$$J_1 = \max_{\omega_g, \zeta_g, i=1,3} \left\{ \frac{\sigma_{d_i}}{\sigma_{x_{3o}}} \right\}, \quad J_2 = \max_{\omega_g, \zeta_g, i=1,3} \left\{ \frac{\sigma_{\ddot{x}_{ai}}}{\sigma_{\ddot{x}_{a3o}}} \right\} \tag{28}$$

J_3 is the criterion calculated from the maximum RMS actuator displacement which provides a measure of the physical size of the control device. The maximum RMS actuator velocity provides a measure of the control power, J_4. The maximum RMS actuator acceleration provides a measure of the magnitude of control forces, J_5.

$$J_3 = \max_{\omega_g, \zeta_g} \left\{ \frac{\sigma_{x_m}}{\sigma_{x_{3o}}} \right\}, \quad J_4 = \max_{\omega_g, \zeta_g} \left\{ \frac{\sigma_{\dot{x}_m}}{\sigma_{\dot{x}_{3o}}} \right\}, \quad J_5 = \max_{\omega_g, \zeta_g} \left\{ \frac{\sigma_{\ddot{x}_{am}}}{\sigma_{\ddot{x}_{a3o}}} \right\} \tag{29}$$

In equations (28) and (29), $\sigma_{x_{3o}} = 1{\cdot}31$ cm, $\sigma_{\dot{x}_{3o}} = 47{\cdot}9$ cm/s and $\sigma_{\ddot{x}_{a3o}} = 1{\cdot}79$ g are the worst-case stationary RMS displacement, velocity and acceleration of the third floor of the uncontrolled building with parameters of $\omega_g = 37{\cdot}3$ rad/s, and $\zeta_g = 0{\cdot}3$. RMS responses are computed using MATLAB/SIMULINK up to 300 s.

Peak responses to El Centro NS and Hachinohe NS earthquake records

The peak responses are calculated from two historical earthquake records, El Centro NS and Hachinohe NS earthquake records, used as the ground excitation. J_6 and J_7 are the criteria calculated from the normalized peak inter-storey drift and acceleration, respectively. The normalized peak displacement, velocity and acceleration of the actuator are evaluated for criteria J_8, J_9, and J_{10}.

$$J_6 = \max_{\substack{t,\, i=1,3 \\ \text{El Centro} \\ \text{Hachinohe}}} \left\{ \frac{|d_i(t)|}{x_{3o}} \right\}, \quad J_7 = \max_{\substack{t,\, i=1,3 \\ \text{El Centro} \\ \text{Hachinohe}}} \left\{ \frac{|\ddot{x}_{ai}(t)|}{\ddot{x}_{a3o}} \right\} \tag{30}$$

$$J_8 = \max_{\substack{t \\ \text{El Centro} \\ \text{Hachinohe}}} \left\{ \frac{|x_m(t)|}{x_{3o}} \right\}, \quad J_9 = \max_{\substack{t \\ \text{El Centro} \\ \text{Hachinohe}}} \left\{ \frac{|\dot{x}_m(t)|}{\dot{x}_{3o}} \right\}, \quad J_{10} = \max_{\substack{t \\ \text{El Centro} \\ \text{Hachinohe}}} \left\{ \frac{|\ddot{x}_{am}(t)|}{\ddot{x}_{a3o}} \right\} \tag{31}$$

Evaluation criteria for the peak responses are non-dimensionalized with respect to the corresponding uncontrolled peak third floor responses. For the El Centro earthquake, $x_{3o} = 3{\cdot}37$ cm, $\dot{x}_{3o} = 131$ cm/s, and $\ddot{x}_{a3o} = 5{\cdot}05$ g. For the Hachinohe Earthquake, $x_{3o} = 1{\cdot}66$ cm, $\dot{x}_{3o} = 58{\cdot}3$ cm/s, and $\ddot{x}_{a3o} = 2{\cdot}58$ g are used.

NUMERICAL RESULTS

Numerical simulations of the proposed GA-based controllers have been performed on the benchmark problem. Two controllers have been developed in this study. They have the same architecture, and have been developed with the same GA parameters and the same fitness and penalty function. However, one has been developed without sensor noise (Case A), and the other considers sensor noise (Case B) while optimizing control gains to improve the robustness of the controller. The measurement noise used in Case B is white noise ranging from $-0{\cdot}1$ to $0{\cdot}1$ V. The RMS noise is $0{\cdot}0577$ V, which is approximately $1{\cdot}9$ per cent of the full span of the A/D converters. It is about $5{\cdot}8$ times larger than the RMS noise used in the bench-mark problem as the implementation constraint.

To develop each controller, only the El Centro earthquake excitation data provided by the benchmark problem has been used. For the state-space reconstruction, the time delay $\tau = 0{\cdot}001$ s has been used in Eq. (14) which is the same as the sampling period in the benchmark problem. MATLAB[15] and SIMULINK[16] have been used for the simulation of the developed controllers. Figures 4 and 5 show the system model and the GA-based controller (Cases A and B) used in this study.

The controlled responses using the GA-based controller (Case A) are compared with the uncontrolled responses under two historic earthquakes—the El Centro and the Hachinohe in Figures 6 and 7, respectively. Controlled responses are reduced by 62 per cent in peak

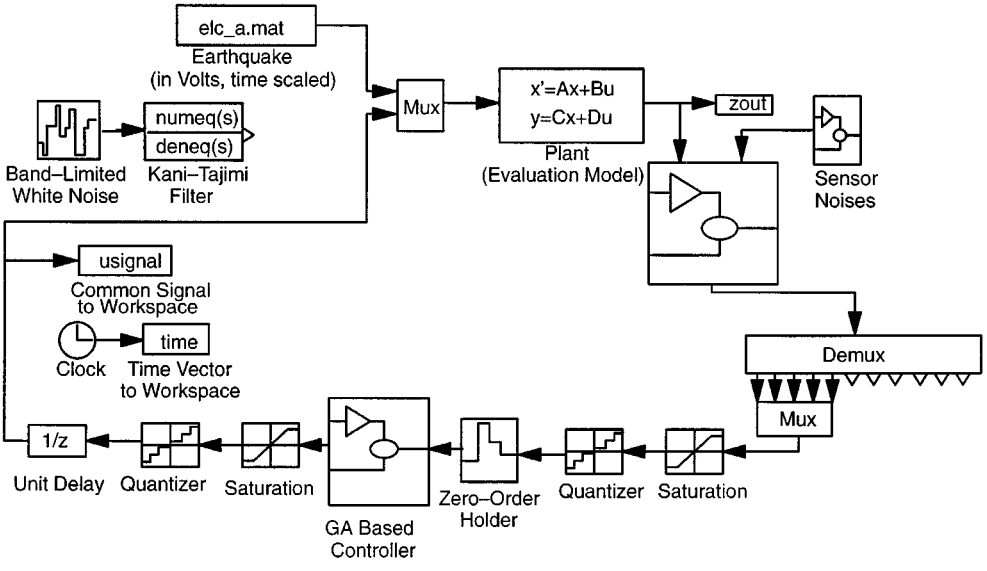

Figure 4. SIMULINK model for the benchmark problem (Cases A and B)

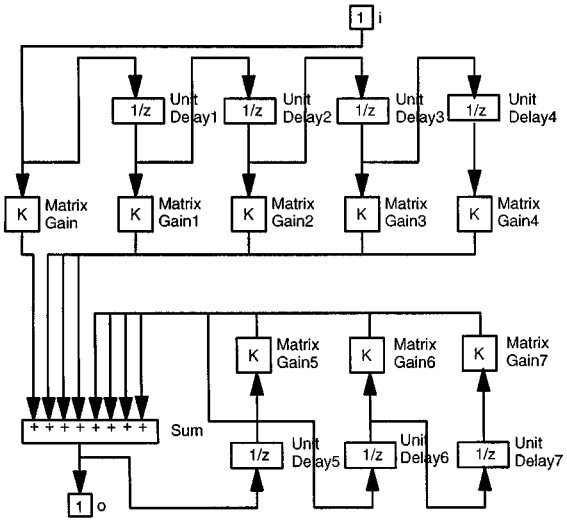

Figure 5. SIMULINK model of GA-based controller (Cases A and B)

displacement and 83 per cent in the RMS value of the displacement compared to uncontrolled responses at the third floor under the El Centro earthquake. Under the Hachinohe earthquake, controlled responses are reduced by 41 per cent in peak displacement and 73 per cent in RMS displacement compared to uncontrolled responses at the third floor. To show the performance

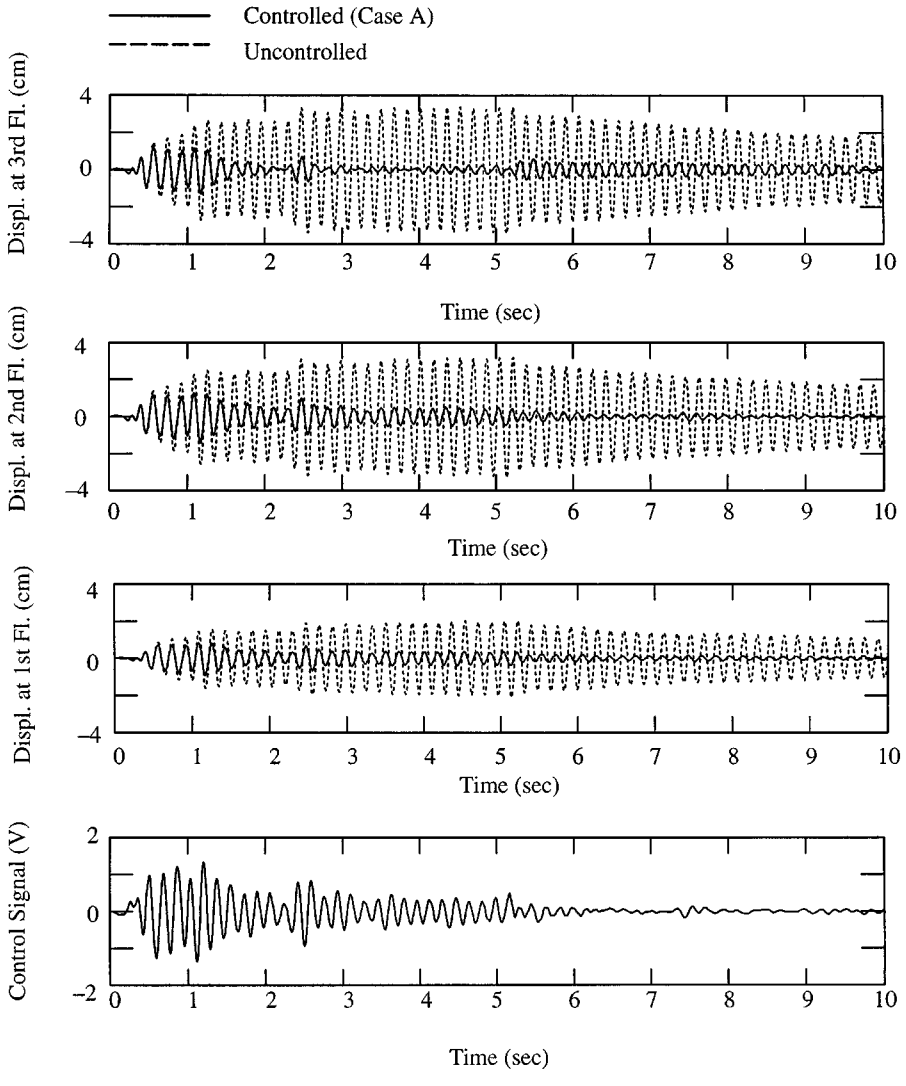

Figure 6. Controlled (Case A) and uncontrolled responses under El Centro earthquake

improvement, these results (Case A) are also compared with the results of the sample LQG control of the benchmark problem. Figure 8 shows that the third floor peak displacement and RMS displacement are 42 and 56 per cent less than the corresponding values in sample LQG controller under the El Centro earthquake. In the Hachinohe earthquake responses, the third floor peak displacement and RMS displacement are reduced by 19 and 44 per cent (Figure 9). Control signals of the GA-based controller and the sample LQG controller are also compared in Figures 8 and 9. Control signals of the GA-based controller are larger than those of the sample LQG when frequencies of the earthquake excitation include the first three lowest frequencies of

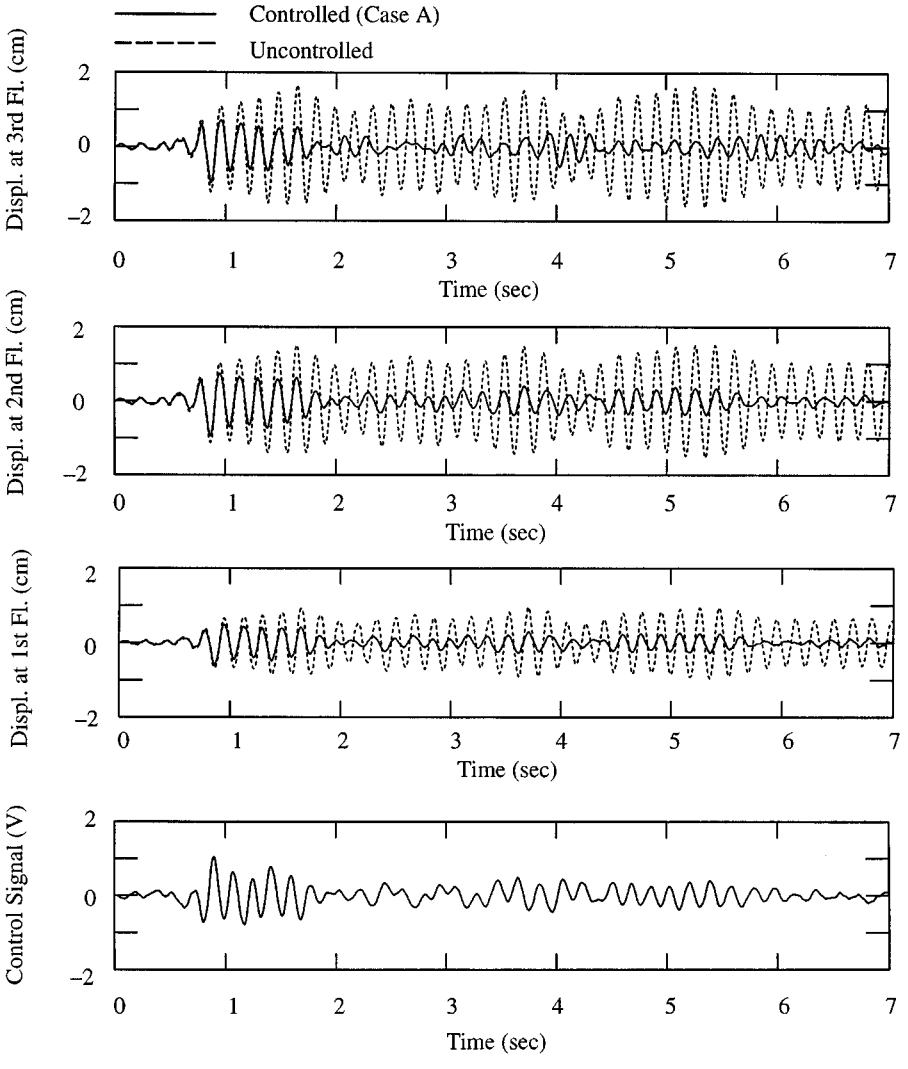

Figure 7. Controlled (Case A) and uncontrolled responses under Hachinohe earthquake

the structure. It is more clear with the frequency response of the controlled structure. Figures 10–12 show the transfer functions from the ground acceleration $\ddot{x}_g$ to absolute accelerations at three floors, $\ddot{x}_{a1}, \ddot{x}_{a2}, \ddot{x}_{a3}$. In these figures, Cases A and B are compared with the uncontrolled results. The GA-based controllers in both cases reduces the response at the first three peaks which are the first three modes of the model structure. In terms of reducing the structural response, the controller in Case A performs better than that in Case B. However, the controller in Case B requires less control effort than Case A. The results of the GA-based control method and its evaluation criteria are listed in Tables I and II (Cases A and B). Both cases satisfy all the constraints in equations (9) and (10).

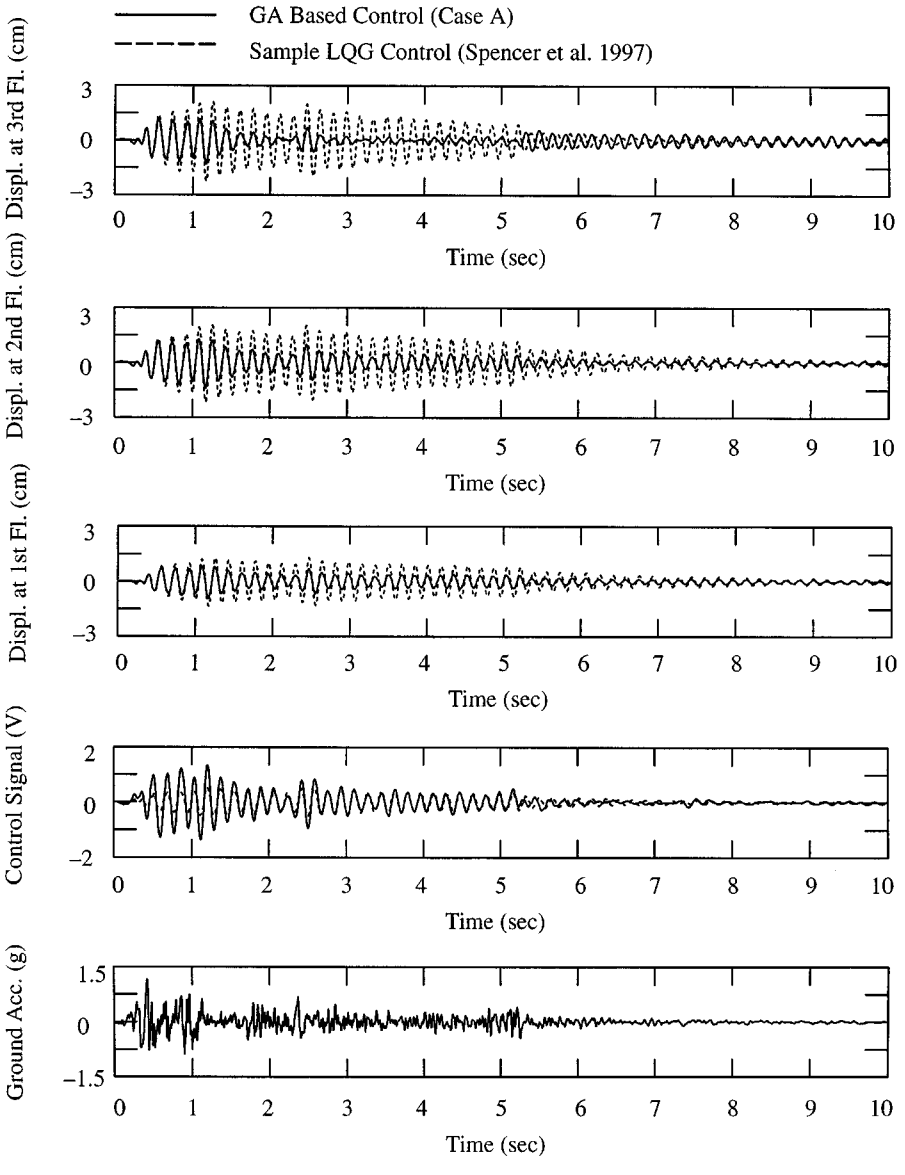

Figure 8. Reponses of GA-based control (Case A) and sample LQG control under El Centro earthquake

The GA-based control method is also compared with several other control methods. The benchmark test results of Covariant Control,[9] Fuzzy control,[7] H_∞ control,[8] LQG method[6] and Sliding Mode Control Methods[10] are compared with the GA-based method in Table III. The results of the proposed GA-based method appear to be comparable with the other methods. Case A is designed to minimize structural responses using the maximum available control effort while

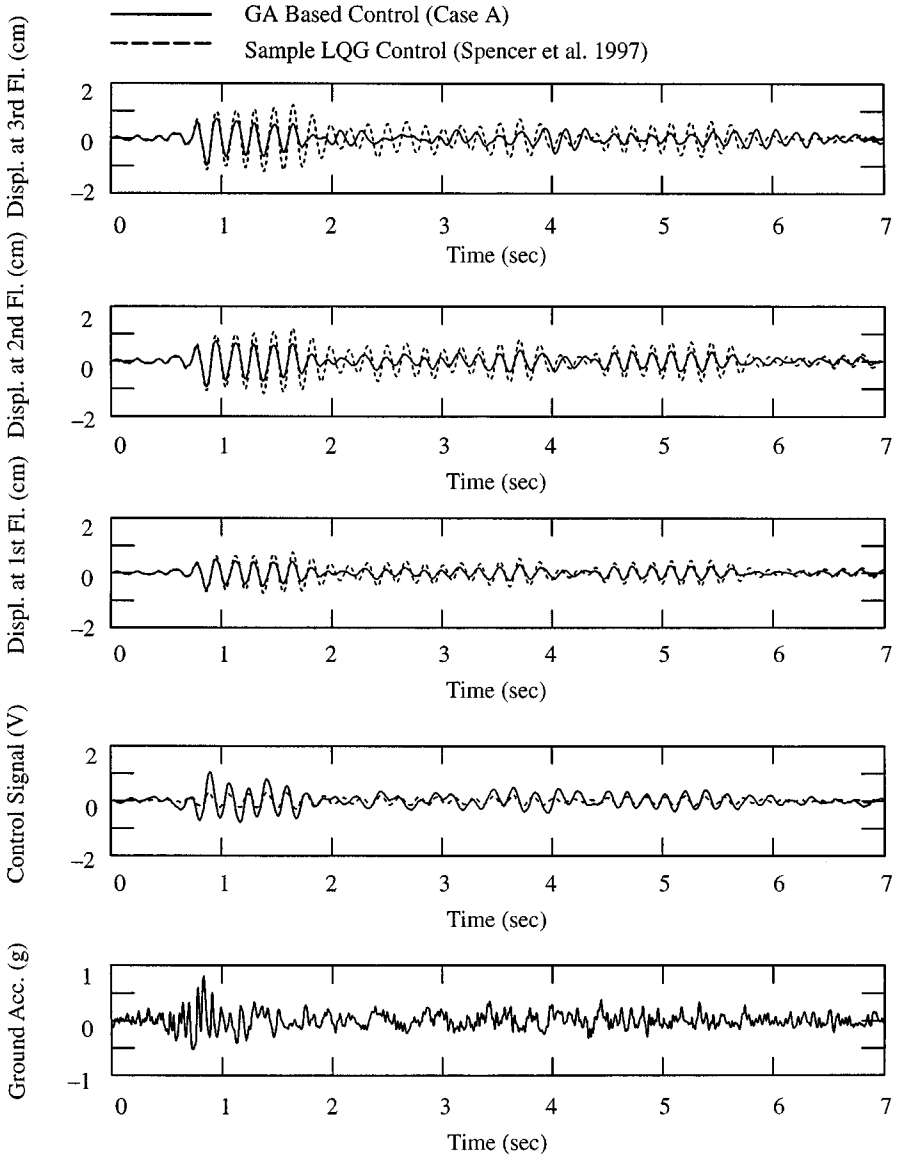

Figure 9. Responses of GA-based control (Case A) and sample LQG control under Hachinohe earthquake

satisfying all of the constraints of the benchmark problem. The results seem to coincide with the design objective.

In practice, it is very difficult to produce an accurately identified model in the high-frequency range where the signal-to-noise ratio is low. The uncertainties in the high frequencies may cause the controller designed from the model to become sensitive and unstable to noise. The frequency

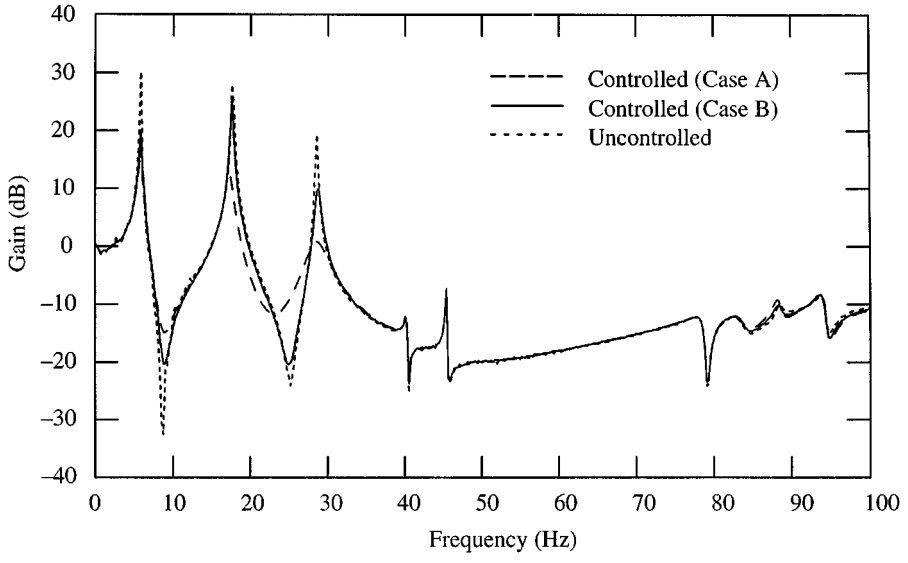

Figure 10. Transfer function from ground acceleration to first floor absolute acceleration

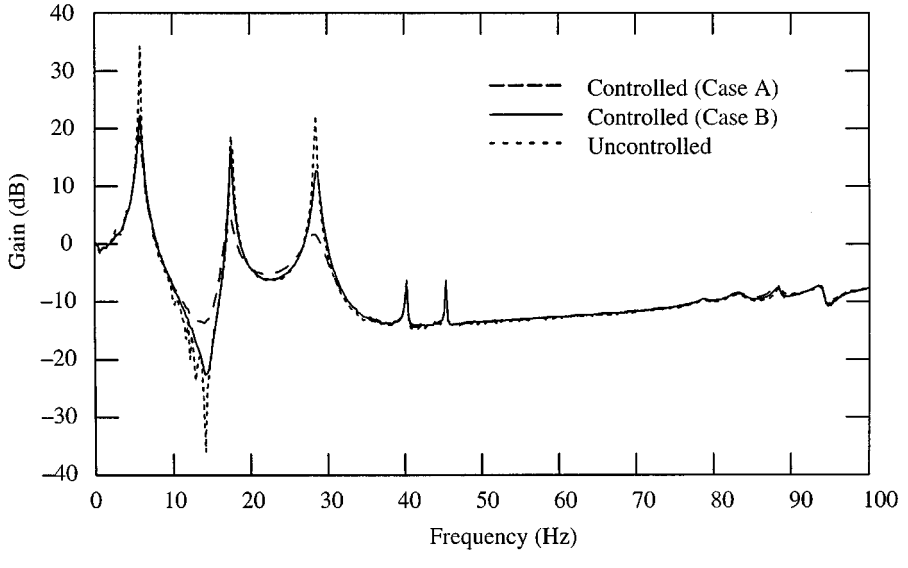

Figure 11. Transfer function from ground acceleration to second floor absolute acceleration

response design method uses the loop gain transfer function to examine the closed-loop stability of the system. The sample LQG controller was considered to be robust in the design if the magnitude of the loop gain was below -5 dB at all frequencies above 35 Hz.[6] The loop gain transfer function of the GA-based controller is calculated by the numerical simulation using

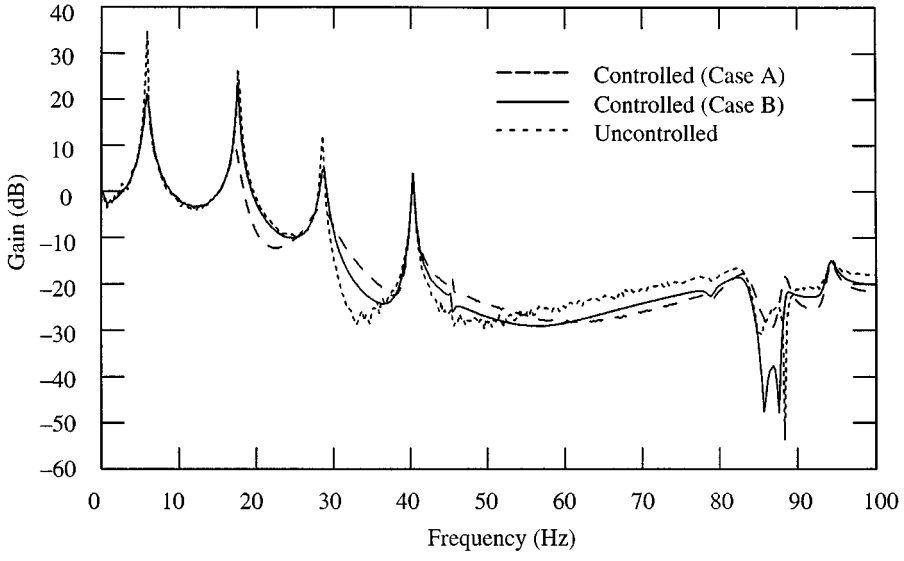

Figure 12. Transfer function from ground acceleration to third floor absolute acceleration

Table I. RMS responses controlled by proposed GA-based strategy (1000 generations)

σ_{d_1}, σ_{d_2}, σ_{d_3} (cm)	0·215* 0·2540†	0·1131* 0·1327†	0·1805* 0·1657†	$\mathbf{J}_1$	0·1642* 0·1939†
$\sigma_{\ddot{x}_{a1}}$, $\sigma_{\ddot{x}_{a2}}$, $\sigma_{\ddot{x}_{a3}}$ (g)	0·3084* 0·3676†	0·4356* 0·5166†	0·4555* 0·5159†	$\mathbf{J}_2$	0·2545* 0·2886†
σ_{x_m}(cm)		1·2522* 1·0573†		$\mathbf{J}_3$	0·9559* 0·8071†
$\sigma_{\dot{x}_m}$(cm/s)		42·897* 36·810†		$\mathbf{J}_4$	0·8956* 0·7685†
$\sigma_{\ddot{x}_{am}}$(g)		1·5585* 1·2451†		$\mathbf{J}_5$	0·8707* 0·6974†
σ_u(V)		0·3235* 0·2751†			

* Case A
† Case B

MATLAB/SIMULINK. The GA-based controller satisfies the same stability and robustness criteria used in the sample LQG controller design in both cases (Figure 13). It can be seen that the robustness is much improved in Case B as expected.

Table II. Peak responses controlled by proposed GA-based strategy (1000 generations)

$\lvert d_1\rvert_{\max}\lvert d_2\rvert_{\max}\lvert d_3\rvert_{\max}$ (cm)	0·9272* 1·0836** 0·5908† 0·6098††	0·5009* 0·5835** 0·3601† 0·3822††	0·5234* 0·4913** 0·2328† 0·2250††	$\mathbf{J}_6$	0·3559† 0·3673††
$\lvert \ddot{x}_{a1}\rvert_{\max}\lvert \ddot{x}_{a2}\rvert_{\max}\lvert \ddot{x}_{a3}\rvert_{\max}$ (g)	1·3820* 1·7112** 1·2270† 1·2712††	1·9461* 2·4074** 1·3536† 1·3345††	1·9430* 2·1961** 1·6114† 1·7365††	$\mathbf{J}_7$	0·6246† 0·6731††
$\lvert x_m\rvert_{\max}$ (cm)		4·9020* 4·2483** 3·7692† 3·0119††		$\mathbf{J}_8$	2·2706† 1·8144††
$\lvert \dot{x}_m\rvert_{\max}$ (cm/sec)		187·36* 157·04** 120·97† 88·40††		$\mathbf{J}_9$	2·0749† 1·5162††
$\lvert \ddot{x}_{am}\rvert_{\max}$ (g)		5·8487* 4·7257** 4·2386† 2·7430††		$\mathbf{J}_{10}$	1·6429† 1·0632††
$\lvert u\rvert_{\max}$ (V)		1·3564* 1·1748** 1·0430† 0·8350††			

El Centro: * Case A ** Case B
Hachinohe: † Case A †† Case B

Table III. Evaluation criteria compared with other optimal control methods

	GA-based control (Case A)	GA-based control (Case B)	Sample LQG Control*	Covariance control* (3rd iteration)	Fuzzy control* (Case B)	H_∞ control* (set S2)	Sliding mode control*
$\mathbf{J}_1$	0·1642	0·1939	0·283	0·2762	0·3232	0·2213	0·1979
$\mathbf{J}_2$	0·2545	0·2886	0·440	0·4205	0·5087	0·3393	0·2936
$\mathbf{J}_3$	0·9559	0·8071	0·510	0·5161	0·4894	0·7054	0·8221
$\mathbf{J}_4$	0·8956	0·7685	0·513	0·5200	0·4137	0·6994	0·8042
$\mathbf{J}_5$	0·8707	0·6974	0·628	0·5001	0·5981	0·7219	0·7775
$\mathbf{J}_6$	0·3559	0·3673	0·456	0·4369	0·4748	0·3859	0·3738
$\mathbf{J}_7$	0·6246	0·6731	0·711	0·6908	0·8666	0·7097	0·6674
$\mathbf{J}_8$	2·2706	1·8144	0·670	0·7197	0·6249	1·0826	1·6832
$\mathbf{J}_9$	2·0749	1·5162	0·775	0·9257	0·6474	1·1078	1·4903
$\mathbf{J}_{10}$	1·6429	1·0632	1·340	1·0589	1·2994	0·9614	1·5673

* Results presented in the Special Issue for the Benchmark Problem in *the Journal of Earthquake Engineering and Structural Dynamics* **27**(11) 1998

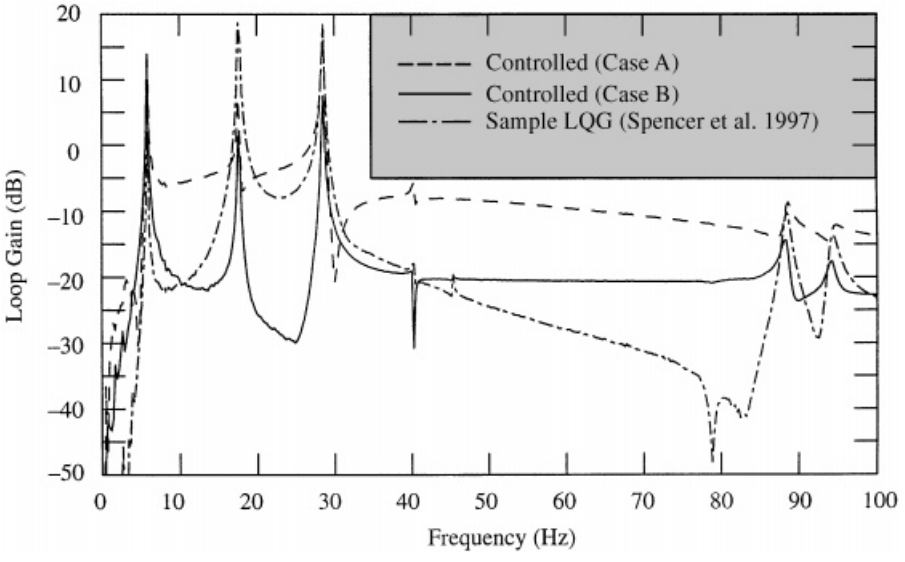

Figure 13. Loop gain transfer function of GA-basesd controller

CONCLUDING REMARKS

In this paper we have proposed a new control method in which the feedback gains are directly optimized by using GAs. We have also proposed a new method of reconstructing the state space from observed time-series responses. The reconstructed state space is used as feedback and the corresponding gains are optimized by GAs.

The advantages of the proposed method are primarily its simplicity and flexibility. The objective function and control constraints can be incorporated into the fitness function. There is considerable flexibility in the formulation of the fitness function, and different weights can be assigned to the objective and constraints in order to fine-tune the control as desired. Another advantage of the proposed method is that it can be easily extended to non-linear control.

The proposed method has been applied to the benchmark problem with two Cases. One has been developed without sensor noise (Case A), and the other considers sensor noises (Case B) while optimizing control gains to improve the robustness of the controller. It is shown that the performance of the proposed GA-based control method is far superior to that of the sample LQG control. We also note that the criteria in sample LQG controller may be different with the control criteria we have used in the GA-based controller. It has also been demonstrated that the performance of the proposed GA-based control method is comparable to several other well-known control methods. The robustness of the GA-based controller has been examined by the loop gain transfer function. The GA-based controller satisfies the same stability and robustness criteria used in the sample LQG controller design in both cases. In Case B the robustness has been much improved by adding measurement noise while optimizing the controller by GAs.

ACKNOWLEDGEMENTS

The research reported in this paper was funded by National Science Foundation Grant CMS-95-003209. This support is gratefully acknowledged.

REFERENCES

1. G. J. Gray, Y. Li, D. J. Murray-Smith and K. C. Sharman, 'Specification of a control system fitness function using constraints of genetic algorithm based design methods', *Proc. 1st Int. Conf. Genetic Algorithms in Eng. Syst.: Innovations and Applications*, 1995, pp. 530–535.
2. D. E. Goldberg, *Genetic Algorithms in Search, Optimization and Machine Learning*, Addison-Wesley, Reading, MA, 1989.
3. S. Kundu and S. Kawata, 'Genetic algorithms for optimal feedback control design', *Engng. Appl. Artif. Intell.* **9**, (4), 403–411 (1996).
4. M. A. Lewis and A. H. Fagg, 'Genetic programming approach to the construction of a neural network for control of a walking robot', *Proc. IEEE Int. Conf. Robot. Automa.*, 1992, pp. 2618–2623.
5. J. Kim, Y. Moon and B. Zeigler, 'Designing fuzzy net controllers using genetic algorithms', *IEEE Control Systems* 66–72 (1995).
6. B. F. Spencer Jr., S. J. Dyke and H. S. Deoskar, 'Benchmark problems in structural control part I: active mass driver systems', *Proc. 1997 ASCE Structures Congress*, April 1997.
7. M. Battaini, F. Casciati and L. Faravelli, 'Fuzzy control of structural vibration. An active mass system driven by a fuzzy controller', *Earthquake Engng. Struct. Dyn.* **27**(11), 1267–1276 (1998).
8. S. E. Breneman and H. A. Smith, 'Design of H_∞ output feedback controllers for the AMD benchmark problem', *Earthquake Engng. Struct. Dyn.* **27**(11), 1277–1289 (1998).
9. J. Lu and R. R. Skelton, 'Covariance control using closed loop modelling for structures', *Earthquake Engng. Struct. Dyn.* **27**(11), 1367–1383 (1998).
10. J. C. Wu, J. N. Yang and A. K. Agrawal, 'Applications of sliding mode control to benchmark problems', *Earthquake Engng. Struct. Dyn.* **27**(11), 1247–1265 (1998).
11. F. Takens, 'Detecting strange attractors in turbulence', Springer Lecture Notes in Mathematics, Vol. 898, Springer, Berlin, 1981, pp. 366–381.
12. A. Langi and W. Kinsner, 'Consonant characterization using correlation fractal dimension for speech recognition', *IEEE WESCANEX 95 Proc.*, 1995, pp. 208–213.
13. S. J. Dyke, B. F. Spencer Jr., P. Quast, D. C. Kaspari Jr. and M. K. Sain, 'Implementation of an active mass driver using acceleration feedback control', *Microcomput. Civil Engng.* **11**, 305–323 (1996).
14. A. Homaifar, C. X. Qi and S. H. Lai, 'Constrained optimization via genetic algorithms', *Simulation* **62**(4), 242–254 (1994).
15. MATLAB, The Math Works Inc., Natick, Massachusetts, 1997.
16. SIMULINK, The Math Works Inc., Natick, Massachusetts, 1997.
17. B. F. Spencer Jr., S. J. Dyke, M. K. Sain and P. Quast, 'Acceleration feedback control strategies for aseismic protection', *Proc. Amer. Control Conf.* 1993, pp. 1317–1321.

